Philippine Journal of Science
153 (3): 885-893, June 2024
ISSN 0031 - 7683
Date Received: 05 Jan 2024

Assessing Solar Radiation Forecasting: a WRF-Solar Model Evaluation in Kupang, Indonesia

Rista Hernandi Virgianto[1]*, Firmansyah[2], and Hamdan Nurdin[3]

[1]Department of Climatology, State School of Meteorology, Climatology, and Geophysics (STMKG), Tangerang Selatan, Banten 15221 Indonesia
[2]Centre For Climate Change Information, Agency for Meteorology, Climatology, and Geophysics (BMKG), Kemayoran, Jakarta 10610 Indonesia
[3]East Nusa Tenggara Climatological Station, Agency for Meteorology, Climatology, and Geophysics (BMKG), Kupang, Nusa Tenggara Timur 85361 Indonesia

In response to the challenges faced by solar power plants in Kupang, Indonesia – particularly during the peak of the rainy season – this study aims to enhance the WRF-Solar (Weather Research and Forecasting–Solar) numerical weather prediction model. Accurate short-term solar radiation forecasting is crucial for managing electricity supply disruptions and controlling operational costs in the City of Kupang and its surroundings. The unpredictable weather patterns – characterized by intense cloud activity during these seasons – pose significant challenges for reliable solar energy generation, thereby making precise weather modeling an essential tool for effective power plant management. Spanning 2020–2022, the research focused on the peak rainy seasons, utilizing a specifically configured WRF-Solar model to simulate solar radiation. Validation of the WRF-Solar model using observational data from the Automatic Solar Radiation Stations at the Kupang Climatological Station showed correlation values consistently above 0.50. However, the model exhibited a tendency to overestimate radiation intensity for GHI and DNI parameters (correlation 0.78 and 0.54) and underestimate for DHI (correlation 0.80), with RMSE values ranging from 47–320 W/m² and MBE values from –41.84 to 116.34 W/m². The model's accuracy was notably higher under clear conditions, with lower RMSE and MBE values but decreased significantly under overcast conditions, hence indicating sensitivity to cloud cover. This study highlights the WRF-Solar model's capability in capturing the diurnal pattern and hourly fluctuations of solar radiation while also underscoring the need for improved cloud representation to enhance accuracy under diverse climatic conditions.

Keywords: daily clearness index, diffuse horizontal irradiance, direct normal irradiance, global horizontal irradiance, solar radiation, WRF-Solar

INTRODUCTION

Global economic growth has led to notable shifts in energy consumption and supply. Energy consumption in Indonesia will rise to 10 kWh/m^2 annually in 2030 (Veanti *et al.* 2022). This forecast underscores the urgency for policymakers to realign economic strategies with sustainable goals. In its 2014 report, the Intergovernmental Panel on Climate Change (IPCC) highlights the energy sector's crucial role in global emissions. This emphasizes the energy sector's centrality in sustainable development strategic revisions (IPCC 2014). The Paris Agreement strengthened the worldwide movement for zero-emissions policy (IPCC 2021).

*Corresponding author: rista.virgianto@stmkg.ac.id

The Indonesian government has for years promoted energy transition policies to increase energy resilience and adapt to climate change, in line with the Paris Agreement. By 2050, the primary energy mix should contain 31% new and renewable energy (Winarno *et al.* 2016). Hardianto (2019) found that Indonesia's solar power development has been slow, with only 95 MW of installed capacity by the end of 2018. The 2019–2028 Government Electricity Supply Business Plan calls for a modest 2-GW expansion by 2028, which is very different from the rest of the world, where solar energy is the fastest-growing renewable energy source.

In Kupang, East Nusa Tenggara is a leader in solar power plant (PLTS in Indonesian) development. Kupang is a desirable location for developing solar energy, especially considering the findings from de Araujo (2020) that indicate high solar radiation levels in nearby East Timor – with measures reaching 1,100 W/m² in October, 1,112 W/m² in November, 1,046 W/m² in December, and 1,077 W/m² in January – hence implying similar potential in Kupang. Solar power generation systems thrive in Kupang due to its climatological characteristics, which include an average dry season of eight months.

Intermittency can lead to less than optimal operations of PLTS due to disruptions in energy source connectivity (Gowrisankaran *et al.* 2016). Intense cloud activity during the rainy season reduces solar energy in certain areas, thereby causing these disruptions (Kuttybay *et al.* 2020). Without adequate assessment, this unpredictability can cause PLTS electrical supply instability (Law *et al.* 2014). Overcast skies during the rainy season can create voltage fluctuations, thereby resulting in equipment damage and higher operational expenses (Bošnjaković *et al.* 2023). Thus, projected solar radiation intensity – especially during the rainy season – is vital for PLTS control to choose the optimal locations for new facilities (Calif *et al.* 2013) and power-generating methods for certain regions (Prasad and Kay 2020).

The WRF-Solar (Weather Research and Forecasting–Solar) model analyzes and predicts solar radiation intensity. This model has been widely used and rigorously tested to simulate solar radiation in Australia (Prasad and Kay 2020), the United States (Jimenez *et al.* 2016), Spain (Arbizu-Barrena *et al.* 2017), South Korea (Kim *et al.* 2017), Singapore (Verbois *et al.* 2018), and Saudi Arabia (Alharbi and Csala 2020). Based on this basis, this research investigates the WRF-Solar model's ability to effectively estimate solar radiation during Kupang's peak rainy season under various cloud cover scenarios. This effort uses advanced WRF-Solar modeling to refine solar radiation forecasts, a crucial step in Indonesian solar energy research for the strategic development of renewable solar resources.

LOCATION AND METHODS

The research takes place in the Kupang region, located in East Nusa Tenggara province, Indonesia. This area, geographically positioned between 10°36'14"S and 10°39'58"S latitude and 123°32'23"E and 123°37'01"E, is renowned for its diverse climatic conditions and unique environmental features. As the provincial capital, Kupang is a central hub for administrative, economic, and cultural activities. The region's tropical savanna climate, marked by extended dry seasons, makes it an ideal site for solar energy research (Suwa 2024).

In this study, solar radiation intensity in Kupang is simulated using the WRF-Solar model. The WRF-Solar model simulations are based on initial condition data from the Final Analysis (FNL) by the National Centers for Environmental Prediction (NCEP). The FNL data, a component of the Global Data Assimilation System, is compiled in real-time from the Global Telecommunication System and includes data from the Global Forecast System. This data – available in GRIB format – offers a temporal resolution of 6 h and a spatial resolution of 1.0° x 1.0°, accessible at https://rda.ucar.edu/datasets/ds083.2/. To perform quantitative validation of the WRF-Solar model outputs, solar radiation data from the Automatic Solar Radiation Stations (ASRS) at the Kupang Climatological Station are utilized. Figure 1 illustrates the simulation domain for the WRF-Solar model – centered at the Kupang Climatological Station at coordinates 10.13861°S and 123.66722°E, with three nested WRF domains.

Parameterization plays a crucial role in representing small-scale meteorological processes and their impact on larger-scale weather phenomena. In weather modeling, parameterization includes various components such as microphysics, cumulus or convection processes, surface land models, the planetary boundary layer (PBL), atmospheric radiation, and physical interactions. A related study by Prasad and Kay (2020) showcased that a specific combination of parameterization schemes Mellor-Yamada-Janjic for the PBL, Kain-Fritsch for cumulus, Unified Noah for the land surface model, along with the Dudhia shortwave and rapid radiative transfer model for longwave radiation (RRTM LW) yielded impressive accuracy in predicting solar radiation intensity under diverse cloud cover conditions. To enhance the representation of cloud activity specific to the research location, adjustments were made to the cumulus and microphysics schemes. This involved integrating the Kain-Fritsch cumulus scheme with the WSM3 microphysics scheme (Sari *et al.* 2018). The Kain-Fritsch cloud parameterization, which employs the air parcel displacement method to address air mass instability, proved effective in reducing overestimated rainfall amounts and refining the accuracy of the predicted

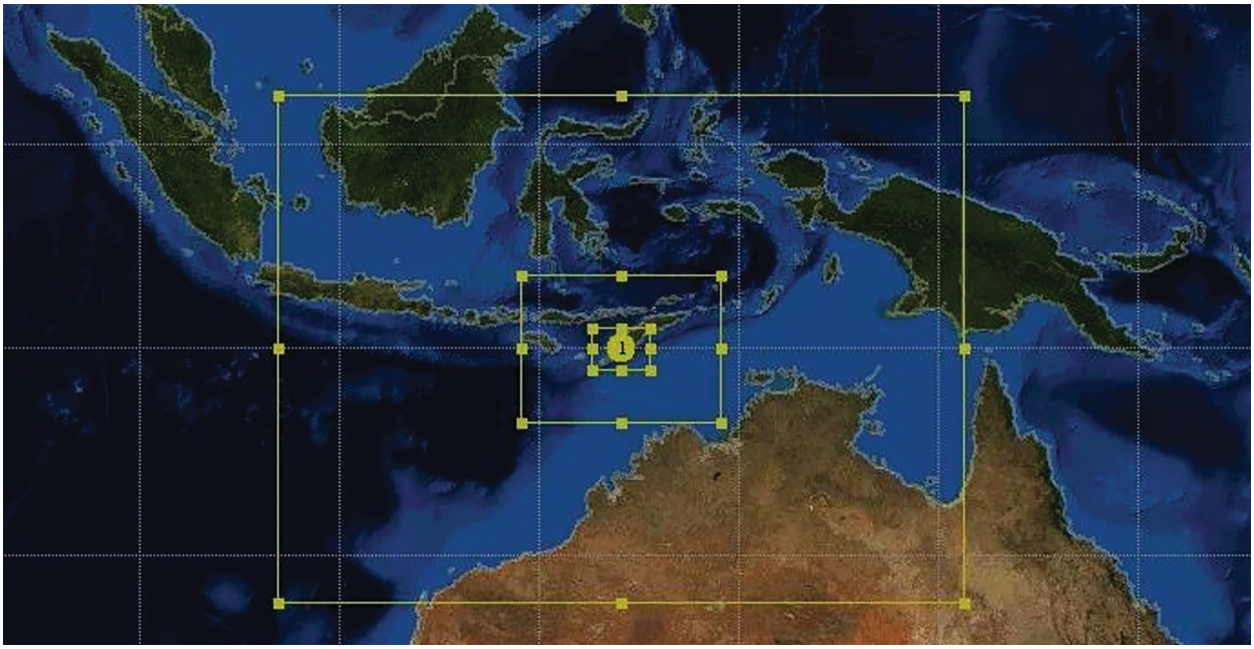

Figure 1. Research location and WRF domains.

radiation intensities (Otieno *et al.* 2020). The detailed configuration of the WRF-Solar model used in this study is presented in Table 1.

Cloud cover conditions in a given region are determined using the daily clearness index (DCI). This index is calculated as the ratio of the sunlight intensity measured on the Earth's surface (S) by observational instruments to the intensity of solar radiation at the top of the atmosphere (TOA, S_O). The DCI effectively illustrates how extraterrestrial solar radiation is attenuated by atmospheric elements, including clouds. In a study by Kim *et al.* (2017), cloud cover is thus classified into three categories based on DCI values – overcast ($0 \leq DCI \leq 0.4$), partly cloudy ($0.4 < DCI \leq 0.7$), and clear ($DCI > 0.7$). The computation of the DCI is performed according to Equation 1 (Soneye 2021):

$$DCI = \frac{S}{S_O} \tag{1}$$

The value of S_O is calculated using Equation 2 (Duffie *et al.* 2020):

$$s_0 = \frac{24}{\pi} i_{sc} \left(1 + 0.044\, cos \frac{360D}{365}\right). (\cos\varphi\ \cos\delta \sin w_s + \frac{2\pi w_s}{360} \sin\varphi sin\ \delta) \tag{2}$$

In this equation, i_{sc} represents the solar constant, which is the amount of solar radiation reaching the outer surface of the Earth – defined as the amount of solar energy arriving at the TOA perpendicular to the incoming solar rays, averaged over the Earth-Sun distance. The commonly used value for the solar constant is 1.367 W/m² (Duffie et al. 2020). The term w_s is the solar hour angle, obtained from Equation 3 (Duffie et al. 2020):

$$w_s = cos^{-1}(-\tan\varphi \tan\delta) \tag{3}$$

Here, δ represents the solar declination angle, and φ is the local latitude. The solar declination angle δ is calculated using Equation 4 (Moukhtar *et al.* 2020):

$$\delta = 23.45\ sin(360\ \frac{284 + Dn}{365}) \tag{4}$$

where Dn is the Julian day, denoting the day number in a year ranging from 1–365.

Table 1. WRF-Solar configurations for each domain.

Configurations	Domain 1	Domain 2	Domain 3
Horizontal grid	100 x 100	88 x 88	76 x 76
Horizontal resolution	27 km	9 km	3 km
Vertical resolution	45 σ levels up to 50hPa		
BDY for meteorology	NCEP FNL at 0,25° × 0,25°		
Microphysics	WRF Single-moment 3-class		
Longwave radiation	Rapid radiative transfer model (RRTMG)		
Shortwave radiation	Dudhia shortwave scheme		
Planetary boundary layer	Yonsei University scheme (YSU)		
Land surface	Unified Noah land surface model		
Cumulus parameterization	Kain-Fritsch		

The ASRS – operated by the Meteorological, Climatological, and Geophysical Agency (BMKG) – measures solar radiation at the Earth's surface encompassing both direct and scattered sunlight. The system primarily concentrates on measuring shortwave solar radiation, utilizing sensors that record data at 10-min intervals to enable accurate and immediate analysis.

Solar radiation is classified into three categories: direct normal irradiance (DNI), diffuse horizontal irradiance (DHI), and global horizontal irradiance (GHI). DNI refers to the direct solar radiation that reaches the Earth's surface, whereas DHI represents the solar radiation that is diffused by atmospheric agents. GHI, on the other hand, represents the total solar radiation, which is the sum of DNI and DHI.

In this study, the WRF-Solar simulation is utilized to simulate GHI, DNI, and DHI during the peak of the rainy season from 2020–2022. The primary goal is to evaluate the model's accuracy in the rainy season's highly variable cloud conditions. The rainy season typically presents significant fluctuations in the DCI due to diverse and frequent cloud cover, hence posing a unique challenge in accurately predicting solar radiation intensity. Thus, this period is ideal for a rigorous test of the WRF-Solar model's performance, especially under conditions of high DCI variability.

To ascertain the accuracy and reliability of the WRF-Solar model's output, this study employs statistical measures for validation: the Pearson correlation coefficient (r), mean bias error (MBE), and root mean square error (RMSE). The Pearson correlation coefficient (r) evaluates the linear relationship between the model's simulated solar radiation data and observed data, whereby a higher "r" value signifies a stronger correlation and higher model accuracy. MBE measures the average bias in the model's predictions, with a lower MBE indicating reduced systematic bias. The RMSE is used to quantify the model's prediction error, thereby providing an understanding of the magnitude of these errors; a lower RMSE suggests greater model accuracy.

Table 2. Daily clearness index (DCI) values during the peak rainy seasons from 2020–2022 in Kupang, Indonesia, categorized by cloud cover conditions.

Date	DCI	Cloud cover condition
2020-12-11	0.74	Clear
2020-12-12	0.62	Partly cloudy
2020-12-13	0.53	Partly cloudy
2020-12-14	0.34	Overcast
2020-12-15	0.53	Partly cloudy
2020-12-16	0.49	Partly cloudy
2020-12-17	0.46	Partly cloudy
2020-12-18	0.46	Partly cloudy
2020-12-19	0.34	Overcast
2020-12-20	0.42	Partly cloudy
2021-01-21	0.72	Clear
2021-01-22	0.56	Partly cloudy
2021-01-23	0.40	Overcast
2021-01-24	0.47	Partly cloudy
2021-01-25	0.36	Overcast
2021-01-26	0.22	Overcast
2021-01-27	0.38	Overcast
2021-01-28	0.42	Partly cloudy
2021-01-29	0.21	Overcast
2021-01-30	0.12	Overcast
2021-01-31	0.29	Overcast
2022-02-21	0.33	Overcast
2022-02-22	0.52	Partly cloudy
2022-02-23	0.12	Overcast
2022-02-24	0.43	Partly cloudy
2022-02-25	0.43	Partly cloudy
2022-02-26	0.09	Overcast
2022-02-27	0.54	Partly cloudy
2022-02-28	0.48	Partly cloudy

RESULTS

Table 2 provides detailed insights into the DCI values during the peak rainy seasons from 2020–2022 in Kupang. In 2020, the DCI values varied, with clear conditions on 11 Dec (DCI = 0.74) and several partly cloudy days like 12 and 13 Dec (DCI values of 0.62 and 0.53, respectively). Overcast conditions were notably present on 14 and 19 Dec, as indicated by lower DCI values of 0.34. In contrast, 2021 started with clear skies on 21 Jan (DCI = 0.72) but soon shifted toward predominantly overcast conditions toward the end of the month, as seen from 23–31 Jan, with the DCI dropping as low as 0.12 on 30 Jan.

The year 2022 continued to exhibit a mix of cloud cover conditions. Overcast days were particularly frequent in February, with the lowest DCI value recorded on the 26 Feb (DCI = 0.09). However, partly cloudy days were also common, as evidenced by DCI values ranging from 0.43–0.54 on several days like 22, 24, 25, 27, and 28 Feb. Throughout these three years, the data demonstrates significant variability in cloud cover – with a higher frequency of partly cloudy days, followed by overcast conditions, and occasional clear skies.

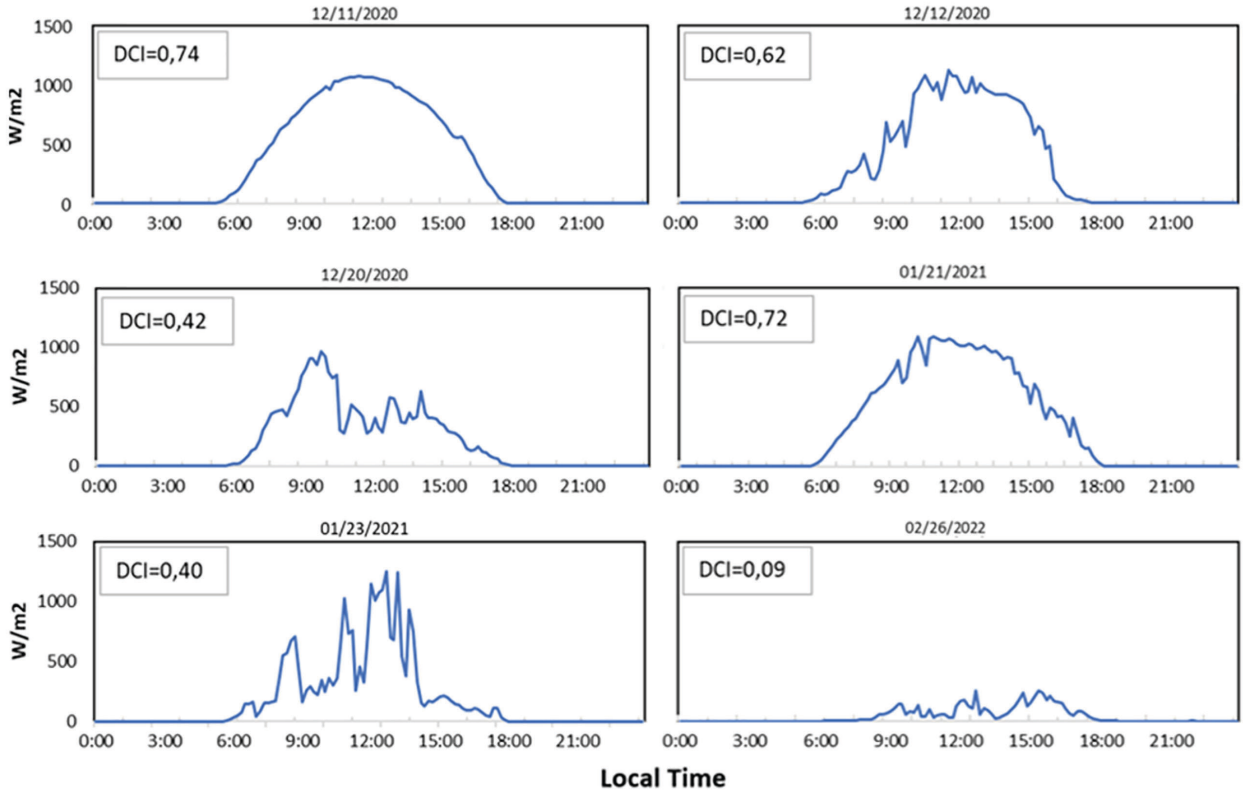

Figure 2. DCI during the peak of the rainy seasons from 2020–2022 at the Kupang climatological station.

Figure 2 presents the characteristic patterns of solar radiation intensity under various cloud cover conditions. On partly cloudy days, there is a significant fluctuation in radiation intensity throughout the day, with the most noticeable fluctuations occurring from late morning to afternoon. During overcast conditions, there is a tendency for the received radiation intensity to decrease over the course of the day. In clear conditions, the pattern of solar radiation intensity shows an increase from 06:00 AM–12:00 PM, peaking at noon, followed by a decrease toward the evening until 06:00 PM.

Based on Table 3, the validation results for solar radiation data – specifically, for the GHI, DHI, and DNI parameters

Table 3. Validation results for solar radiation indexes (*i.e.* GHI, DHI, and DNI) under different cloud cover conditions in Kupang, Indonesia.

Index	Cloud cover	RMSE (W/m^2)	MBE (W/m^2)	r
GHI	All conditions	214.04	37.94	0.78
	Overcast	251.98	96.46	0.72
	Partly cloudy	192.36	2.63	0.83
	Clear	112.45	–43.76	0.97
DHI	All conditions	112.46	–41.84	0.80
	Overcast	107.12	–25.33	0.74
	Partly cloudy	124.11	–61.14	0.85
	Clear	47.20	0.97	0.86
DNI	All conditions	289.75	116.34	0.54
	Overcast	320.28	156.03	0.42
	Partly cloudy	278.74	103.11	0.57
	Clear	153.06	–26.00	0.92

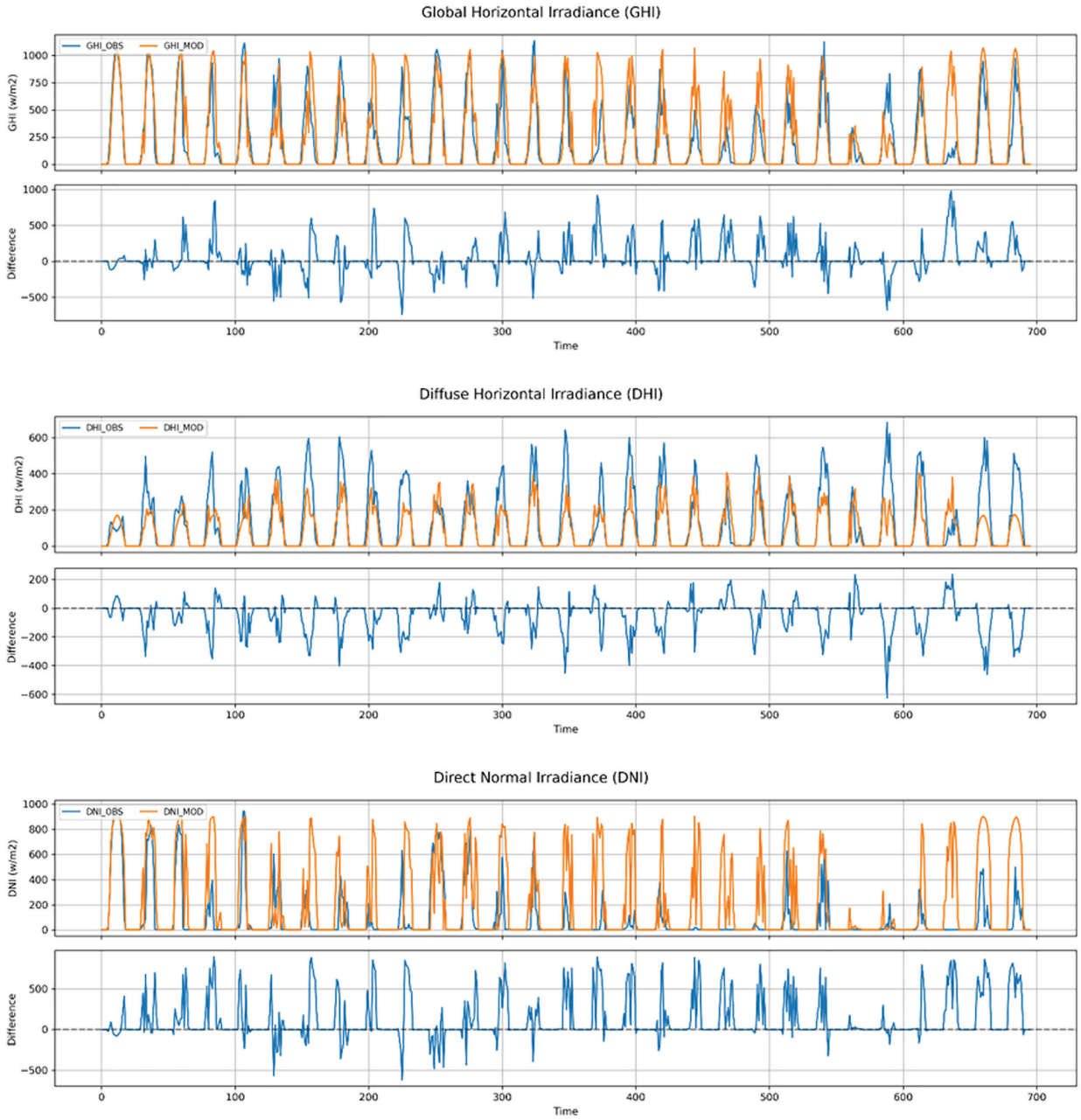

Figure 3. Temporal comparison of hourly GHI and DNI radiation simulations from WRF-Solar against ASRS observation during the peak of rainy seasons from 2020–2022 at Kupang climatological station.

under various cloud cover conditions – demonstrate varying levels of accuracy. The highest accuracy is observed during simulations in clear conditions, whereas the accuracy of the WRF-Solar model significantly decreases under overcast conditions. For the GHI radiation parameter across all cloud cover conditions, a correlation value of 0.78 was achieved, along with an RMSE of 214.0 W/m² and an MBE of 37.94 W/m². As for the DHI radiation parameter, the calculations yielded a correlation of 0.80, an RMSE of 112.5 W/m², and an MBE of –41.84 W/m². Furthermore, for the DNI parameter, the correlation value was 0.54 – with an RMSE of 289.75 W/m² and an MBE of 116.34 W/m².

Figure 3 presents a comparison of the patterns of solar radiation intensity from WRF-Solar outputs with ASRS observational data. It can be observed in the figure that for the GHI and DNI parameters, the intensity of radiation produced tends to be overestimated compared to observational data. In contrast, for the DHI parameter, the solar radiation intensity pattern shows values that

are underestimated in comparison to observational data. In general, the model has successfully captured the diurnal pattern of daily radiation intensity and its hourly fluctuations.

DISCUSSION

The variability in DCI values, with an average of 0.41, classifies the majority of observed conditions as "partly cloudy." This aligns with the findings of Kim *et al.* (2017) and highlights the small but significant impact of cloud cover on the amount of solar radiation received. On clear days, radiation patterns were shown to be predictable, thus suggesting that there was minimal influence from clouds. Partially cloudy and overcast situations revealed large radiation intensity changes, which is important for solar power generation because extensive cloud cover lowers DCI values and reduces solar radiation intensity at the surface (Zhang and Ma 2020).

Our study demonstrates improved solar radiation simulation accuracy – with RMSE values of 214.0 W/m² for GHI, 112.5 W/m² for DHI, and 289.75 W/m² for DNI. The model effectively simulates solar radiation variations in highly variable cloud conditions. Prasad and Kay (2020) found higher RMSE values under complex and highly fluctuating atmospheric conditions, hthus indicating greater solar irradiance simulation discrepancies. Although our results indicate an advancement in the prediction of solar radiation, the practicality of our model may be constrained by geographical and climatic factors.

Model accuracy decreases under overcast conditions, hence highlighting the need for improved cloud representation in the WRF-Solar model. Errors in cloud prediction, including incorrect estimations of cloud formation and movement, have a substantial impact on simulation results. Consequently, this factor is vital for enhancing the accuracy of forecasts. The inaccuracies arise from possible discrepancies in the model's parameterization schemes – specifically, in representing the microphysical processes of cloud formation and the dynamics of the PBL, which are essential to accurately simulating atmospheric conditions (Gueymard and Jimenez 2018; Prasad and Kay 2020).

In atmospheric circulation, surface variables and the boundary layer interact to transfer heat, moisture, and momentum (Zhang *et al.* 2013). The surface-PBL heat exchange drives circulation and convection, thereby affecting cloud formation and movement over time (Chiacchio and Vitolo 2012). Concurrently, atmospheric circulation and the delicate equilibrium of energy on Earth are sustained through the interaction between clouds and radiation. Energy transmission to the surface is influenced by the processes of cloud formation, whereas the pressure and altitude of clouds are determined by circulation.

Additional analysis shows that model simulation errors generally correspond with atmospheric humidity and temperature, which affect cloud formation and movement. These characteristics affect the stability of the atmospheric column and, as a result, impact the likelihood of convection and the formation of clouds (Prasad and Kay 2020). Another study also highlighted the sensitivity of the diurnal cloud cycle to wind intensity, which drives thermal lifting and mechanically induced lifting, thereby triggering convection (Houze 2012). Errors in these domains could affect actual conditions, thereby resulting in inconsistencies between the observed and simulated cloud cover, as well as the intensity of solar radiation

To improve the precision of the WRF-Solar model in cloudy conditions, it is necessary to specifically improve the way cloud parameters are represented. This involves refining the cloud physics schemes to better capture the processes of cloud formation and dissipation. Sub-grid scale cloud feedback mechanisms can improve the model's cloud cover response by better representing cloud dynamics. Additionally, for accurate simulations of cloud behavior, it is vital to refine cloud microphysics processes and enhance the modeling of boundary layer inversions and turbulence.

CONCLUSION

The research conducted in Kupang from 2020–2022 incorporating the WRF-Solar model with specific configurations – microphysics (WRF Single-moment 3-Class), longwave radiation [rapid radiative transfer model (RRTMG)], shortwave radiation (Dudhia shortwave scheme), PBL [Yonsei University scheme (YSU)], land surface (unified Noah land surface model), and cumulus parameterization (Kain-Fritsch) – has yielded crucial insights into the effects of cloud cover variability on solar radiation.

These findings, based on DCI values, highlight the model's ability to track daily fluctuations in solar radiation intensity. However, the accuracy of these predictions varies with the degree of cloudiness – performing best under clear skies but diminishing as cloud cover intensifies, with the most significant drop in precision on overcast days. Model predictions for solar radiation parameters – including GHI, DHI, and DNI – demonstrate a strong correlation (above 0.50) with actual observational data, spanning RMSE values from 47–320 W/m². The model exhibits a systematic bias under varying cloud conditions, thereby leading to overestimations for GHI

and DNI while underestimating DHI.

This investigation reveals that although the WRF-Solar model is generally adept at simulating solar radiation, discrepancies under cloudier conditions highlight the necessity for ongoing improvements in cloud interaction modeling to refine solar radiation forecasting accuracy. Such enhancements are critical for regions with diverse cloud cover. Continuous model refinement and comprehensive validation are indispensable for delivering precise solar energy forecasts, which are essential for effective energy resource management and strategic planning across various climates.

ACKNOWLEDGMENTS

The authors extend their gratitude to the State School of Meteorology, Climatology, and Geophysics Indonesia for their indispensable funding and support. We also thank the BMKG for providing the essential data that greatly contributed to this research. Our appreciation is also extended to our colleagues for their valuable insights and contributions.

STATEMENT ON CONFLICT OF INTEREST

The authors declare that there are no conflicts of interest regarding the publication of this paper.

REFERENCES

ALHARBI F, CSALA D. 2020. Saudi Arabia's solar and wind energy penetration: future performance and requirements. Energies 13: 588.

ARBIZU-BARRENA C, RUIZ-ARIAS JA, RODRÍGUEZ-BENÍTEZ FJ, POZO-VÁZQUEZ D, TOVAR-PESCADOR J. 2017. Short-term solar radiation forecasting by advecting and diffusing MSG cloud index. Solar Energy 155: 1092–1103.

BOŠNJAKOVIĆ M, STOJKOV M, KATINIĆ M, LACKOVIĆ I. 2023. Effects of Extreme Weather Conditions on PV Systems. Sustainability 15: 16044.

CALIF R, SCHMITT FG, HUANG Y, SOUBDHAN T. 2013. Intermittency study of high frequency global solar radiation sequences under a tropical climate. Solar Energy 98: 349–365.

CHIACCHIO M, VITOLO R. 2012. Effect of cloud cover and atmospheric circulation patterns on the observed surface solar radiation in Europe. Journal of Geophysical Research: Atmospheres, Vol. 117.

DE ARAUJO JMS. 2020. A Case Study: Performance Comparison of Solar Power Generation between GridLAB-D and SAM in Dili, Timor Leste. Journal of Power and Energy Engineering 8: 1.

DUFFIE JA, BECKMAN WA, BLAIR N. 2020. Solar engineering of thermal processes, photovoltaics, and wind. John Wiley & Sons.

GOWRISANKARAN G, REYNOLDS SS, SAMANO M. 2016. Intermittency and the value of renewable energy. Journal of Political Economy 124: 1187–1234.

GUEYMARD C, JIMENEZ P. 2018. Validation of real-time solar irradiance simulations over Kuwait using WRF-Solar. 12th International Conference on Solar Energy for Buildings and Industry (EuroSun2018); Rapperswil, Switzerland.

HARDIANTO H. 2019. Utilization of solar power plant in Indonesia: a review. International Journal of Environment, Engineering and Education 1: 1–8.

HOUZE JR. RA. 2012. Orographic effects on precipitating clouds. Reviews of Geophysics 50.

[IPCC] Intergovernmental Panel on Climate Change. 2014. Mitigation of Climate Change. Contribution of Working Group III to the Fifth Assessment Report of the Intergovernmental Panel on Climate Change. Geneva.

[IPCC] Intergovernmental Panel on Climate Change. 2021. AR6 Climate Change 2021: the physical science basis. Geneva.

JIMENEZ PA, HACKER JP, DUDHIA J, HAUPT SE, RUIZ-ARIAS JA, GUEYMARD CA, THOMPSON G, EIDHAMMER T, DENG A. 2016. WRF-Solar: description and clear-sky assessment of an augmented NWP model for solar power prediction. Bulletin of the American Meteorological Society 97: 1249–1264.

KIM J-Y, YUN C-Y, KIM CK, KANG Y-H, KIM H-G, LEE S-N, KIM S-Y. 2017. Evaluation of WRF model-derived direct irradiance for solar thermal resource assessment over South Korea. AIP Conference Proceedings 2017. AIP Publishing.

KUTTYBAY N, SAYMBETOV A, MEKHILEF S, NURGALIYEV M, TUKYMBEKOV D, DOSYMBETOVA G, MEIIRKHANOV A, SVANBAYEV Y. 2020. Optimized single-axis schedule solar tracker in different weather conditions. Energies 13: 5226.

LAW EW, PRASAD AA, KAY M, TAYLOR RA. 2014. Direct normal irradiance forecasting and its application to concentrated solar thermal output forecasting – a review. Solar Energy 108: 287–307.

MOUKHTAR I, EL DEIN AZ, ELBASET AA, MITANI Y. 2020. Solar Energy: Technologies, Design, Modeling, and Economics. Springer Nature.

OTIENO G, MUTEMI J, OPIJAH F, OGALLO L, OMONDI M. 2020. The sensitivity of rainfall characteristics to cumulus parameterization schemes from a WRF model. Part I: A case study over East Africa during wet years. Pure and Applied Geophysics 177: 1095–1110.

PRASAD AA, KAY M. 2020. Assessment of simulated solar irradiance on days of high intermittency using WRF-Solar. Energies 13: 385.

SARI FP, BASKORO AP, HAKIM OS. 2018. Effect of different microphysics scheme on WRF model: a simulation of hail event study case in Surabaya, Indonesia. AIP Conference Proceedings 2018. AIP Publishing.

SONEYE OO. 2021. Evaluation of clearness index and cloudiness index using measured global solar radiation data: a case study for a tropical climatic region of Nigeria. Atmósfera 34: 25–39.

SUWA T. 2024. Prediction of latent heat storage transient thermal performance for integrated solar combined cycle using machine learning techniques. Journal of Energy Storage 76: 109856.

VEANTI DPO, VIRGIANTO RH, ASTIDUARI IGAPP. 2022. The Impact of Climate Change on Cooling Energy Demand in Indonesia Based on Representative Concentration Pathways (RCP) Scenarios. Science and Technology Indonesia 7: 9–16.

VERBOIS H, HUVA R, RUSYDI A, WALSH W. 2018. Solar irradiance forecasting in the tropics using numerical weather prediction and statistical learning. Solar Energy 162: 265–277.

WINARNO OT, ALWENDRA Y, MUJIYANTO S. 2016. Policies and strategies for renewable energy development in Indonesia. 2016 IEEE International Conference on Renewable Energy Research and Applications (ICRERA) 2016. p. 270–272.

ZHANG G, MA Y. 2020. Clear-sky surface solar radiation and the radiative effect of aerosol and water vapor based on simulations and satellite observations over Northern China. Remote Sensing 12: 1931.

ZHANG H, PU Z, ZHANG X. 2013. Examination of errors in near-surface temperature and wind from WRF numerical simulations in regions of complex terrain. Weather and Forecasting 28: 893–914.